Eur. J. Mineral., 37, 761–772, 2025 https://doi.org/10.5194/ejm-37-761-2025 © Author(s) 2025. This work is distributed under the Creative Commons Attribution 4.0 License.





Suenoite, □Mn₂Mg₅Si₈O₂₂(OH)₂, a new member of the amphibole supergroup from the Scortico–Ravazzone ore deposit (Apuan Alps, Tuscany, Italy)

Cristian Biagioni^{1,2}, Elena Bonaccorsi^{1,2}, Marco Pasero^{1,2}, Ulf Hålenius³, and Ferdinando Bosi⁴

¹Dipartimento di Scienze della Terra, Università di Pisa, Via Santa Maria 53, 56126 Pisa, Italy ²Centro per l'Integrazione della Strumentazione scientifica dell'Università di Pisa, Università di Pisa, Pisa, Italy ³Department of Geosciences, Swedish Museum of Natural History, Box 50007, 10405 Stockholm, Sweden ⁴Dipartimento di Scienze della Terra, Sapienza Università di Roma, Piazzale Aldo Moro 5, 00185 Rome, Italy

Correspondence: Cristian Biagioni (cristian.biagioni@unipi.it)

Received: 6 April 2025 - Revised: 27 July 2025 - Accepted: 30 July 2025 - Published: 20 October 2025

Abstract. Suenoite (IMA 2019-075), ideally $\Box Mn_2Mg_5Si_8O_{22}(OH)_2$, is a new member of the amphibole supergroup discovered in the Mn ore deposit of Scortico–Ravazzone, Apuan Alps, Tuscany, Italy. It occurs as colourless tabular striated crystals, up to 0.1 mm in length, associated with spessartine and baryte. The streak is white, and the lustre is vitreous. Mohs hardness is estimated between 5.5 and 6. Cleavage is perfect on {210}. The calculated density is 3.283 g cm⁻³. Suenoite is optically biaxial (+), with $\alpha = 1.655(5)$, $\beta = 1.660(5)$, and $\gamma = 1.670(5)$ (in white light). $2V_{\text{meas}}$ is $75(10)^\circ$, and $2V_{\text{calc}}$ is 70.9° . The orientation is X = a, Y = b, and Z = c. Pleochroism was not observed, as suenoite is colourless. The empirical chemical formula of suenoite is $A(\Box_{0.91}Ca_{0.07}Na_{0.02})_{\Sigma 1.00} B(Mn_{1.64}^{2+}Fe_{0.36}^{2+})_{\Sigma 2.00} C(Mg_{3.56}Fe_{0.91}^{2+}Mn_{0.61}^{2+}Zn_{0.02})_{\Sigma 5.10} T(Si_{7.86}Al_{0.06})_{\Sigma 7.92} O_{22} W[(OH)_{1.92}F_{0.08}]_{\Sigma 2.00}$, and it is based on electron microprobe analyses, infrared spectroscopy, and Mössbauer spectroscopy. The unit-cell parameters of suenoite are $\alpha = 18.7508(12)$, $\alpha = 18.1396(12)$, $\alpha = 18.1$

1 Introduction

Minerals of the amphibole supergroup are based on the general formula $AB_2C_5T_8O_{22}W_2$, where $A = \square$, Na^+ , K^+ , and Pb^{2+} ; $B = Na^+$, Ca^{2+} , Mn^{2+} , Fe^{2+} , Mg^{2+} , and Li^+ ; $C = Mg^{2+}$, Fe^{2+} , Mn^{2+} , Al^{3+} , Fe^{3+} , Mn^{3+} , Cr^{3+} , V^{3+} , Ti^{4+} , and Li^+ ; $T = Si^{4+}$, Al^{3+} , and Be^{2+} ; and $W = (OH)^-$, F^- , Cl^- , and O^{2-} (Hawthorne et al., 2012).

Among the 118 minerals currently recognised as valid species within the amphibole supergroup (IMA List of Minerals – updated September 2025; available at http://cnmnc.units.it/, last access: 3 October 2025), only a few have Mn^{2+} as a species-forming constituent. Ferrighoseite, $\square(NaMn^{2+})(Mg_4Fe^{3+})Si_8O_{22}(OH)_2$ (e.g. Oberti and Ghose, 1993; Banno et al., 2019), and hjalmarite,

Na(NaMn²⁺)Mg₅Si₈O₂₂(OH)₂ (Holtstam et al., 2019), both belong to the sodium–(magnesium–iron–manganese) amphibole subgroup and are characterised by the valency-imposed double site occupancy (NaMn²⁺) at the M(4) site. Manganoferri-eckermannite, NaNa₂(Mn₄²⁺Fe³⁺)Si₈O₂₂(OH)₂ (e.g. Nambu et al., 1969; Barkley et al., 2010), belongs to the sodium amphibole subgroup, whereas mangano-manganiungarettiite, NaNa₂(Mn₂²⁺Mn₃³⁺)Si₈O₂₂O₂ (Hawthorne et al., 1995a; Oberti et al., 2017), belongs to the oxo-amphibole group, in which Mn²⁺ is the dominant divalent cation among C cations.

The first description of an amphibole having solely Mn^{2+} as B cation was made by Sueno et al. (2002). The mineral, with end-member composition $\Box Mn_2^{2+}Fe_5^{2+}Si_8O_{22}(OH)_2$,

was approved under the name protomangano-ferroanthophyllite. That name soon became incorrect: in fact, after the IMA report on the amphibole supergroup (Hawthorne et al., 2012), the prefix mangano- must indicate the dominance of $\mathrm{Mn^{2+}}$ among C cations, and the composition $\mathrm{\Box Mn_2^{2+}Fe_5^{2+}Si_8O_{22}(OH)_2}$ deserves a distinct root name.

The root name "suenoite" was adopted for minerals having Mn^{2+} as the *B* dominant constituent (Williams et al., 2013). That name was intended as a posthumous recognition to Shigeho Sueno (1937–2011), late professor of mineralogy at the University of Tsukuba, Japan, who described protomangano-ferro-anthophyllite. This mineral has been renamed to proto-ferro-suenoite, where the prefix proto- refers to the protoamphibole structure with space group *Pnmn*, and the prefix ferro- indicates the dominant divalent *C* cation. More recently, the minerals clino-suenoite, $\Box Mn_2^{2+}Mg_5Si_8O_{22}(OH)_2$, and clino-ferro-suenoite, $\Box Mn_2^{2+}Fe^{2+}Si_8O_{22}(OH)_2$, have been described (Oberti et al., 2018; Holtstam et al., 2024). Here the prefix clino- refers to the clinoamphibole structure with space group C2/m.

We herewith describe the new mineral suenoite. The lack of any structural prefix (proto- or clino-) refers to the anthophyllite-like orthoamphibole structure with space group Pnma. The new mineral and its name have been approved by the IMA Commission on New Minerals, Nomenclature and Classification (proposal IMA # 2019-075). The name follows the general guidelines on the nomenclature of amphiboles. In fact, Mg^{2+} , as the dominant divalent C cation, and $(OH)^-$, as the dominant W anion, do not require any adjectival prefix. Holotype material is deposited in the mineralogical collection of the Museo di Storia Naturale, Università di Pisa, Via Roma 79, Calci (PI), Italy, under catalogue number 19 891.

2 Occurrence and physical properties

Suenoite was identified in a specimen provided by the mineral collector Tiberio Bardi and sampled in an outcrop located between the collapsed adits at 1074 and 1052 m above sea level, respectively, of the Scortico-Ravazzone Mn ore deposit (latitude 44°07′39″ N, longitude 10°07′12″ E), Fivizzano, Apuan Alps, Massa Carrara, Tuscany, Italy. This deposit is hosted within an upper Mesozoic metasedimentary sequence formed by quartzites, calcschists, phyllites, and marbles. Previous studies reported the occurrence of spessartine, tephroite, rhodonite, pyroxmangite, rhodochrosite, quartz, friedelite, probable sonolite, and an amphibolesupergroup mineral (Di Sabatino, 1967; Abrecht, 1989). Recent investigations improved upon this mineral list through the identification of alabandite, alleghanvite, baryte, calcite, fluorite, galena, hausmannite, hübnerite, magnetite, malachite, manganosite, melanostibite, pyrite, pyrolusite, sarki-

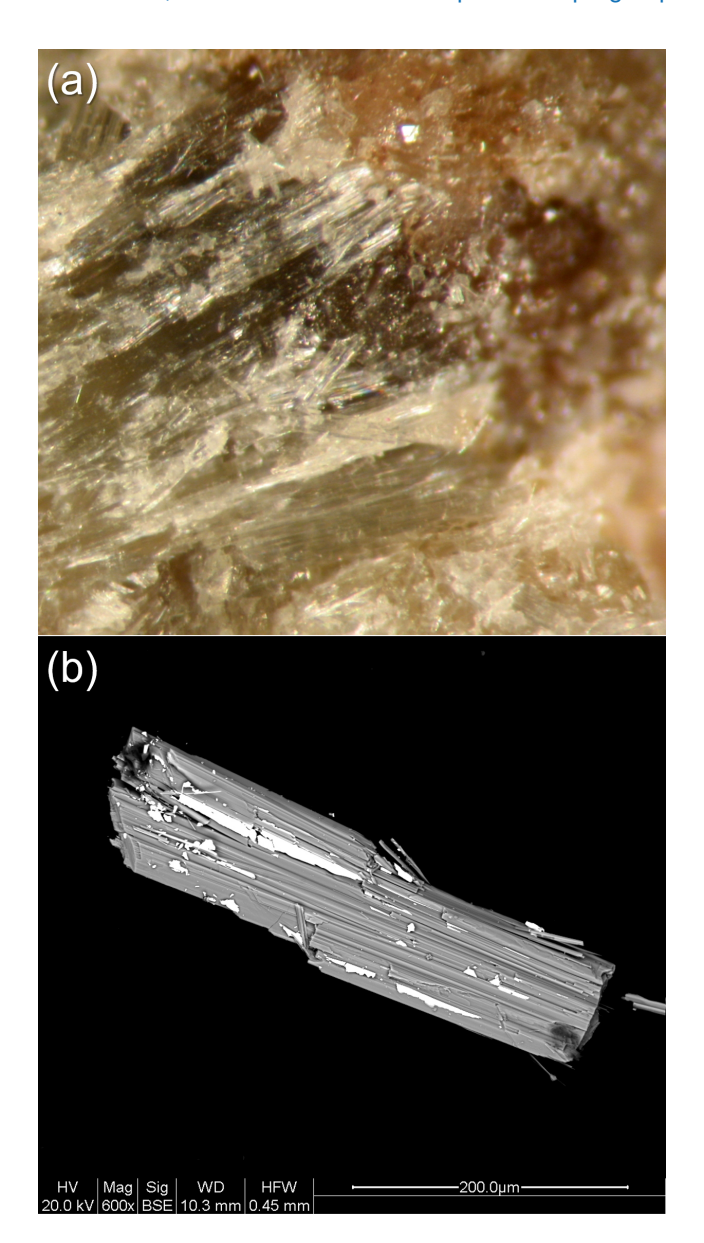


Figure 1. Colourless fibrous crystals of suenoite with spessartine (a) (field of view: 2 mm) and a backscattered electron image (b) showing a fibrous crystal of suenoite (grey) closely associated with baryte (white). Scortico–Ravazzone, Fivizzano, Massa-Carrara, Tuscany, Italy. Holotype material.

nite, sonolite, sphalerite, welinite, and the new mineral species scorticoite (Biagioni et al., 2019; Musetti et al., 2022).

Suenoite occurs as tabular striated crystals up to 0.1 mm in size (Fig. 1). It is colourless, with a white streak and a vitreous lustre. It is brittle, with perfect {210} cleavage and a fracture that is irregular. Hardness and density were not measured owing to the small size of the available material. However, a Mohs hardness between 5.5 and 6 could be estimated by analogy with other amphibole-supergroup minerals. The calculated density is 3.283 g cm⁻³, based on the empirical

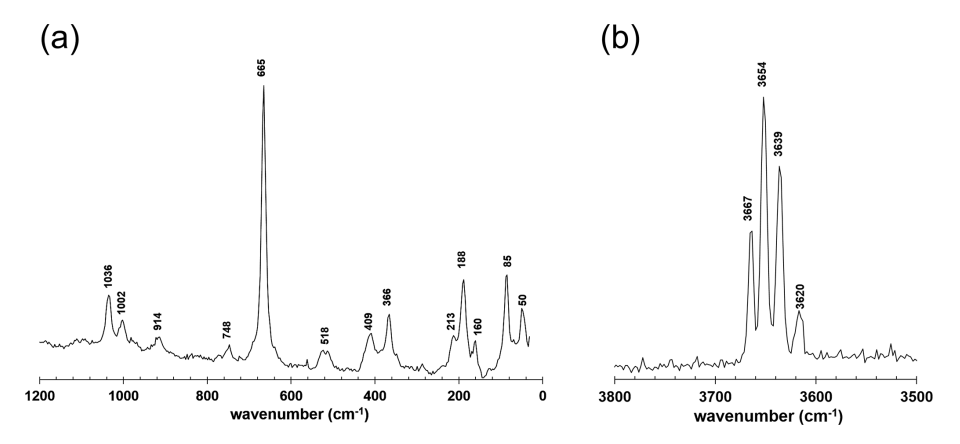


Figure 2. Raman spectrum of suenoite in the range $1200-30 \,\mathrm{cm}^{-1}$ (a) and $3800-3500 \,\mathrm{cm}^{-1}$ (b).

formula and unit-cell volume refined from single-crystal X-ray diffraction data. Suenoite is transparent. It is biaxial (+), with $\alpha=1.655(5)$, $\beta=1.660(5)$, and $\gamma=1.670(5)$ (in white light). $2V_{\rm meas}$ is $75(10)^\circ$, and $2V_{\rm calc}$ is 70.9° . The orientation is X=a, Y=b, and Z=c. Pleochroism was not observed, as suenoite is colourless. The compatibility index $[1-(K_P/K_C)]$ is 0.009, well within the "superior" range (Mandarino, 1981).

In type material suenoite is associated with spessartine and baryte. Its origin is probably related to the recrystallisation of the Scortico–Ravazzone Mn ore deposit during the Tertiary tectono-metamorphic events affecting the rocks belonging to the Alpi Apuane metamorphic complex.

3 Spectroscopic analyses

3.1 Raman spectroscopy

Micro-Raman spectra were obtained on an unpolished sample of suenoite in nearly backscattered geometry with a Jobin-Yvon Horiba XploRA apparatus, equipped with a motorised x-y stage and an Olympus BX41 microscope with a $10\times$ objective (Dipartimento di Scienze della Terra, University of Pisa, Pisa, Italy). The 532 nm line of a solid-state laser was used. The minimum lateral and depth resolution was set to a few μ m. The system was calibrated using the 520.6 cm⁻¹ Raman band of silicon before each experimental session. Spectra were collected through multiple acquisitions with single counting times of 60 s. Backscattered radiation was analysed with a 1200 grooves mm⁻¹ grating monochromator.

Figure 2 shows the Raman spectrum of suenoite. The region between 1200 and $30\,\mathrm{cm}^{-1}$ is shown in Fig. 2a. According to Waeselmann et al. (2019), the Mg–Fe–Mn amphiboles have pronounced Raman scattering below $100\,\mathrm{cm}^{-1}$. These authors also proposed that the Raman peak occurs at ca. 80--85 and $60\text{--}70\,\mathrm{cm}^{-1}$ in monoclinic and orthorhombic amphiboles, respectively. However, in suenoite, a sharp

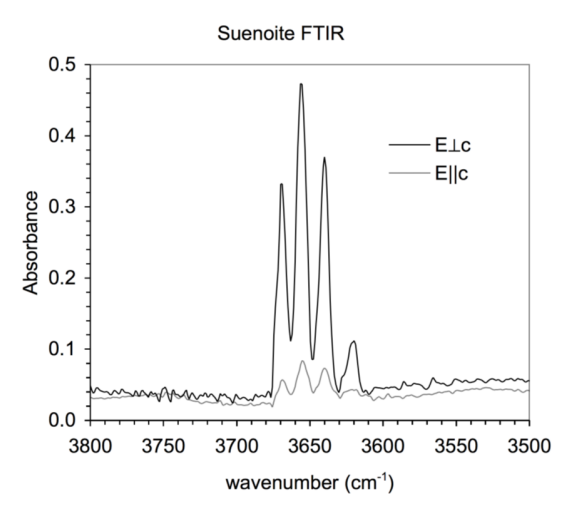


Figure 3. FTIR spectra of suenoite in the OH-stretching region.

Raman band occurs at 85 cm⁻¹. The presence of a Raman signal was observed with the c axis parallel and perpendicular to the polarisation direction of the incident laser, in agreement with other orthorhombic amphiboles. An additional band occurs at 50 cm⁻¹. The strongest Raman feature is a band at 665 cm⁻¹, related to the stretching modes of T-O-T bonds. The slight shift of the band position at wavenumbers lower than 670 cm⁻¹ can be attributed to the occurrence of ^CFe²⁺ and minor ^TAl (Waeselmann et al., 2019). The band at $1036 \,\mathrm{cm}^{-1}$ is able to give some information about the ^CFe²⁺ content and its distribution between the M1 and M3 sites. Using the relations proposed by Waeselmann et al. (2019) for ^CMn-free amphiboles, a total amount of ^CFe²⁺ of 1.32(8) atoms per formula unit (apfu) can be predicted, with ${}^{M1,M3}\text{Fe}^{2+} = 0.93$ apfu. Consequently, ${}^{M2}\text{Fe}^{2+}$ may be 0.39(5) apfu. These data have to be compared with the results of Mössbauer spectroscopy and crystal-structure refinement (see below). In the region of the O-H stretching modes (Fig. 2b), four strong bands occur due to different lo-

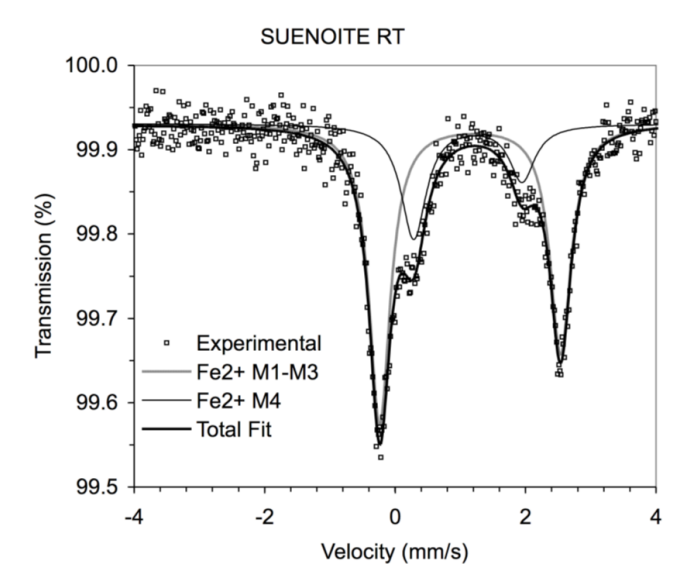


Figure 4. Room temperature Mössbauer spectrum of suenoite.

cal atomic arrangements, in line with those observed through infrared spectroscopy.

3.2 Infrared spectroscopy

Polarised FTIR absorption spectra (Fig. 3) were measured on holotype material (36 µm thick prismatic grain) using a Bruker Vertex spectrometer equipped with a Hyperion II microscope, a Globar source, a KBr beam splitter, and an MCT detector (Department of Geosciences, Swedish Museum of Natural History, Stockholm, Sweden). Data were acquired during 128 scans in the wavenumber range 6000–600 cm⁻¹ with a resolution of 2 cm⁻¹.

Bands occur at 3674 (shoulder), 3669, 3657, 3640, and 3620 cm⁻¹. These bands can be assigned to different local atomic arrangements around OH3A and OH3B. In agreement with Hawthorne and Della Ventura (2007), let us consider the site configuration symbol M1M1M3-O3-A:T1T1-M2M2M3. This symbol was proposed for monoclinic amphiboles but can be modified and applied to orthorhombic amphiboles. In suenoite, A and T sites can be considered occupied by \(\Price \) and Si only, respectively, neglecting minor Na, Ca, and Al. In addition, very minor F replacing OH can be neglected. Bands at 3674 and 3669 cm⁻¹ are likely related to tremolite-like arrangements, i.e. Mg-MgMg. The slight shift of the band at 3669 cm⁻¹ may be related to the replacement of Ca^{2+} by $(Mn,Fe)^{2+}$ at M4. The band at $3657 \,\mathrm{cm}^{-1}$ may be related to the atomic arrangement $MgMgM^{2+}$, where $M^{2+} = Fe$, Mn, neglecting minor Zn. Finally, the bands at 3640 and 3620 cm⁻¹ can be due to the arrangements MgM²⁺M²⁺ and M²⁺M²⁺, respectively.

Table 1. Mössbauer hyperfine parameters for suenoite.

I %	$\frac{\text{CS}}{(\text{mm s}^{-1})}$	$QS \pmod{s^{-1}}$	$\begin{array}{c} \text{FWHM} \\ (\text{mm s}^{-1}) \end{array}$	Assignment
72(3)	1.15(1)	2.77(1)	0.39(2)	$M1-M3_{Fe}^{2+}$
28(3)	1.12(1)	1.66(5)	0.46(6)	$M4_{Fe}^{2+}$

Table 2. Chemical data (in wt %) for suenoite.

Constituent	Mean	Range	$SD(\sigma)$
SiO ₂	52.89	49.79–54.97	1.63
Al_2O_3	0.33	0.06 - 1.19	0.30
MgO	16.08	14.88-17.49	0.84
CaO	0.46	0.34 - 0.73	0.11
MnO	17.84	16.01-19.88	1.26
FeO _{tot}	10.20	9.40-11.03	0.55
ZnO	0.18	0.12 - 0.22	0.03
Na ₂ O	0.07	0.03 - 0.11	0.03
F	0.18	0.04 - 0.28	0.07
H_2O_{calc}	1.94		
Subtotal	100.17		·
O = F	-0.08		
Total	100.09		

3.3 Mössbauer spectroscopy

The Mössbauer spectrum of suenoite (Fig. 4) was collected at room temperature in transmission mode using a ⁵⁷Co point source in the Rh matrix with a nominal activity of 10 mCi (Department of Geosciences, Swedish Museum of Natural History, Stockholm, Sweden). The Mössbauer spectrum was acquired during 16 d over the velocity range $\pm 4 \,\mathrm{mm \, s^{-1}}$ and was calibrated against α -Fe foil. The Mössbauer absorber consisted of a few mg of carefully selected amphibole grains, which were axially pressed onto a $\sim 1.5 \,\mathrm{mm}^2$ area of a mylar window. This absorber preparation resulted in a preferred orientation of the fibrous to long prismatic mineral grains and caused intensity asymmetry of the recorded Mössbauer quadrupole doublets. The spectrum could be adequately fitted with two quadrupole doublets using the programme MossA (Prescher et al., 2012), resulting in the hyperfine parameters given in Table 1. In agreement with previous assignments of quadrupole doublets observed in Mössbauer spectra of amphibole-supergroup species (e.g. Hawthorne, 1988), the outer doublet with a quadrupole splitting of $2.77 \,\mathrm{mm}\,\mathrm{s}^{-1}$ is assigned to Fe^{2+} at the M1-M3 sites, and the inner doublet with a quadrupole splitting of 1.66 mm s⁻¹ is assigned to Fe^{2+} at the M4 site. No absorption related to Fe^{3+} was observed in the recorded spectrum. Due to the limited amount of pure suenoite crystal fragments available, the absorption of the present spectrum is merely 0.4%, and for this reason the signal-to-noise ratio is of medium quality even after more than 2 weeks of data acquisition. Consequently, small

Table 3. X-ray powder diffraction data (d in Å) for suenoite.

$I_{ m obs}$	$d_{ m obs}$	$I_{\rm calc}$	$d_{ m calc}$	hkl	I _{obs}	$d_{ m obs}$	$I_{ m calc}$	$d_{ m calc}$	hkl
m	9.1	48	9.07	020	_	_	5	2.368	650
S	8.4	100	8.33	210		2.212	18	2.341	5 5 1
	5 10	7	5.12	101	W	2.312	6	2.313	7 2 1
W	5.10	6	5.08	230			6	2.292	461
_	_	8	4.92	1 1 1			10	2.261	271
_	_	7	4.62	201	w	2.187	23	2.169	502
***	4.54	12	4.535	040			9	2.154	5 1 2
W	4.34	10	4.482	2 1 1	w	2.166	23	2.152	5 6 1
W	4.16	16	4.164	420		1.979	16	2.011	661
W	3.914	11	3.905	1 3 1	W	1.979	8	1.997	7 5 1
W	3.675	36	3.674	2 3 1	_	_	9	1.887	702
m	3.322	17	3.365	3 3 1	W	1.855	5	1.849	642
G	3.263	15	3.279	4 2 1	w	1.055	6	1.846	8 5 1
S	3.203	44	3.259	4 4 0	w	1.749	6	1.749	861
VS	3.085	71	3.080	610	w	1.716	6	1.701	033
		7	3.040	4 3 1	w	1./10	5	1.697	282
mw	2.932	19	2.903	5 2 1			6	1.640	902
m	2.851	40	2.855	2 5 1	mw	1.632	16	1.633	961
-	_	12	2.776	630			14	1.625	2 11 0
m	2.727	7	2.734	5 3 1	mw	1.596	20	1.593	053
111	2.121	44	2.702	3 5 1	W	1.565	6	1.563	1200
m	2.615	32	2.603	161	W	1.531	14	1.526	10 6 1
		7	2.583	621	w	1.331	5	1.524	163
m	2.537	37	2.558	202	mw	1.514	14	1.512	0 12 0
111	2.331	15	2.531	261	111 W	1.514	17	1.509	263
		24	2.525	4 5 1	W	1.460	5	1.458	6 11 0
W	2.442	24	2.447	3 0 2	W	1.432	7	1.435	11 0 2

Intensity and d_{hkl} were calculated using PowderCell 2.3 software (Kraus and Nolze, 1996) on the basis of the structural model given in Table 5. Only the reflections with $I_{\rm calc} > 5$ are given, if not observed. Intensities were visually estimated: vs – very strong, s – strong, m – medium, mw – medium weak, w – weak. The eight strongest reflections are given in bold.

amounts (less than 5 % of the total iron content of the sample) of Fe^{3+} cannot be entirely ruled out. However, as amphiboles with mixed iron valences are in general strongly green to blue in colour due to Fe^{2+} – Fe^{3+} intervalence charge transfer absorption that occurs in the red portion of the visible spectrum, the colourless nature of suenoite strongly suggests that it is indeed virtually free from Fe^{3+} .

4 Chemical analysis

Quantitative chemical analyses of suenoite were obtained by an electron microprobe using a Cameca SX50 instrument (Istituto di Geologia Ambientale e Geoingegneria, CNR, Rome, Italy), operating in WDS mode at 15 kV with a sample current of 15 nA and a beam diameter of 1 µm. The following standards were used: jadeite (Na), periclase (Mg), orthoclase (K), rutile (Ti), wollastonite (Si and Ca), metallic Zn (Zn), fluorphlogopite (F), corundum (Al), rhodonite (Mn), and magnetite (Fe). K, Ti, and Cr were sought but found to be below the detection limit. The PAP routine was applied (Pouchou and Pichoir, 1985) for correction of the recorded

raw data. Chemical data are given in Table 2 (n = 12 spot analyses).

The empirical formula of suenoite, based on 24 anions per formula unit (pfu) and partitioning Fe as B and C constituents according to Mössbauer data, is ${}^A(\Box_{0.91}\mathrm{Ca}_{0.07}\mathrm{Na}_{0.02})_{\Sigma1.00}$ ${}^B(\mathrm{Mn}_{1.64}^{2+}\mathrm{Fe}_{0.36}^{2+})_{\Sigma2.00}$ ${}^C(\mathrm{Mg}_{3.56}\mathrm{Fe}_{0.91}^{2+}\mathrm{Mn}_{0.61}^{2+}\mathrm{Zn}_{0.02})_{\Sigma5.10}$ ${}^T(\mathrm{Si}_{7.86}\mathrm{Al}_{0.06})_{\Sigma7.92}$ ${}^O(\mathrm{C}_{22})_{W}[(\mathrm{OH})_{1.92}\mathrm{Fo}_{0.08}]_{\Sigma2.00}.$ The simplified formula of suenoite is $(\Box,\mathrm{Ca})(\mathrm{Mn},\mathrm{Fe})_2(\mathrm{Mg},\mathrm{Fe},\mathrm{Mn})_5\mathrm{Si}_8\mathrm{O}_{22}[(\mathrm{OH}),\mathrm{F}]_2.$ The ideal formula of suenoite is $\Box\mathrm{Mn}_2\mathrm{Mg}_5\mathrm{Si}_8\mathrm{O}_{22}(\mathrm{OH})_2,$ which requires (in wt%) SiO₂ 57.08, MgO 23.93, MnO 16.85, and H₂O 2.14.

5 X-ray crystallography

Powder X-ray diffraction data of suenoite (Table 3) were collected using a 114.6 mm Gandolfi camera with Ni-filtered $CuK\alpha$ radiation (Dipartimento di Scienze della Terra, University of Pisa, Pisa, Italy). Owing to the multiplicity of indices of several reflections, unit-cell parameters were not refined.

Table 4. Crystal and experimental data for suenoite.

Crystal data	
Crystal size (mm)	$0.15 \times 0.10 \times 0.04$
Crystal system, space group	Orthorhombic, Pnma
a (Å)	18.7508(12)
b (Å)	18.1396(12)
c (Å)	5.3173(3)
$V(Å^3)$	1808.6(2)
Z	4
Data collection and refinement	
Radiation, wavelength (Å)	Mo <i>K</i> α, 0.71073
Temperature (K)	293(2)
$2\theta_{\rm max}$ (°)	60.00
Measured reflections	33 439
Unique reflections	2725
Reflections with $F > 4\sigma F$	2236
R _{int}	0.0456
$R\sigma$	0.0205
Range of h, k, l	$-26 \le h \le 26$
	$-25 \le k \le 25$
	$-7 \le l \le 7$
$R[F > 4\sigma F]$	0.0490
R (all data)	0.0597
wR (on F^2)	0.1163
Goodness of fit	1.096
Number of least-squares parameters	194
Maximum and	0.83 (at 0.88 Å from O4B)
minimum residual peak ($e \text{Å}^{-3}$)	-1.26 (at 0.71 Å from H3B)

A single-crystal X-ray diffraction study was carried out using a Bruker Smart Breeze diffractometer equipped with a Photon II CCD area detector and graphite-monochromatised $MoK\alpha$ radiation (Dipartimento di Scienze della Terra, University of Pisa, Pisa, Italy). The detector-to-crystal distance was 50 mm. Data were collected using ω scan mode, in 0.5° slices, with an exposure time of 45 s per frame. The data were corrected for Lorentz and polarisation factors and absorption using the software package Apex3 (Bruker AXS Inc., 2016).

The crystal structure of suenoite was refined using Shelxl-2018 (Sheldrick, 2015) starting from the atomic coordinates of anthophyllite (Walitzi et al., 1989). The statistical tests on the distribution of |E| values and the systematic absences agree with the space group Pnma. The following neutral scattering curves, taken from the International Tables for Crystallography (Wilson, 1992), were used: Mn vs. Mg at M4, Mg vs. Fe at M1-M3, Si at the T sites, O at the O sites, and H at the H sites. An anisotropic structural model converged to $R_1=0.0490$ for 2236 unique reflections with $F>4\sigma(F)$ and 194 refined parameters. Details of data collection and refinement are given in Table 4. Atom coordinates and equivalent isotropic displacement parameters are reported in Table 5. Table 6 reports selected bond distances and Table 7 the site scattering and proposed site populations; the latter were

obtained by distributing the ions of the formula unit among the M sites under the constraint of the refined site-scattering values (Hawthorne et al., 1995b), the mean bond lengths, and Mössbauer data. In agreement with Oberti et al. (2018), Mn was preferentially hosted at M4 together with minor Fe^{2+} , as indicated by Mössbauer spectroscopy; the Mn excess was assigned to the M1 site, in agreement with the preference of Mn for this site with respect to M2 and M3. Bond-valence calculations, weighted according to the proposed site populations and obtained using the bond-valence parameters of Brese and O'Keeffe (1991), are reported in Table 8. The crystal structure of suenoite is shown in Fig. 5.

6 Discussion

6.1 Crystal chemical features

The general features of the crystal structure of suenoite are the same as those of the orthorhombic *Pnma* species belonging to the amphibole supergroup (e.g. Hawthorne and Oberti, 2007) and are not detailed here. Its structural formula can be written as ${}^A\Box^{M4}(Mn_{1.64}Fe_{0.36})_{\Sigma 2.00}$ ${}^{M1-M3}(Mg_{3.55}Fe_{0.85}Mn_{0.60})_{\Sigma 5.00}Si_8O_{22}$ (OH)₂.

Table 5. Sites, site occupancy (s.o.), fractional atom coordinates, and isotropic (*) or equivalent isotropic displacement parameters (in \mathring{A}^2) for suenoite.

Site	s.o.	x/a	y/b	z/c	$U_{ m eq/iso}$
M4	Mn _{0.954(7)} Mg _{0.046(7)}	0.12334(3)	-0.01269(3)	0.39347(11)	0.00842(18)
M1	Mg _{0.637(6)} Fe _{0.363(6)}	0.12501(5)	0.16262(4)	0.39280(15)	0.0054(3)
M2	Mg _{0.796(6)} Fe _{0.204(6)}	0.12519(5)	0.07213(5)	-0.10583(18)	0.0056(3)
M3	Mg _{0.735(8)} Fe _{0.265(8)}	0.12537(7)	1/4	-0.1079(2)	0.0060(4)
T1A	Si _{1.00}	0.23193(5)	-0.16569(5)	-0.43745(18)	0.0039(2)
T1B	Si _{1.00}	0.01780(5)	-0.16617(5)	0.27182(18)	0.0039(2)
T2A	Si _{1.00}	0.22806(5)	-0.08015(5)	0.05903(17)	0.0045(2)
T2B	Si _{1.00}	0.02354(5)	-0.08144(5)	-0.22546(18)	0.0049(2)
O1A	$O_{1.00}$	0.18204(14)	0.16331(14)	0.0569(5)	0.0063(5)
O1B	$O_{1.00}$	0.06817(14)	0.16301(14)	-0.2718(5)	0.0074(5)
O2A	$O_{1.00}$	0.18561(14)	0.07697(14)	-0.4365(5)	0.0071(5)
O2B	$O_{1.00}$	0.06293(14)	0.07680(14)	0.2225(5)	0.0083(5)
OH3A	$O_{1.00}$	0.1818(2)	1/4	-0.4417(7)	0.0087(7)
OH3B	$O_{1.00}$	0.0691(2)	1/4	0.2277(7)	0.0079(7)
O4A	$O_{1.00}$	0.18783(14)	-0.00277(14)	0.0721(5)	0.0079(5)
O4B	$O_{1.00}$	0.06424(14)	-0.00540(14)	-0.2795(5)	0.0096(5)
O5A	$O_{1.00}$	0.19925(14)	-0.12059(14)	0.3223(5)	0.0078(5)
O5B	$O_{1.00}$	0.05007(14)	-0.11559(14)	0.0449(5)	0.0076(5)
O6A	$O_{1.00}$	0.20168(14)	-0.12857(14)	-0.1817(5)	0.0078(5)
O6B	$O_{1.00}$	0.04861(14)	-0.13514(16)	-0.4617(5)	0.0107(5)
O7A	$O_{1.00}$	0.2042(2)	1/3	0.5460(7)	0.0090(7)
O7B	$O_{1.00}$	0.0459(2)	1/3	0.2358(7)	0.0092(7)
H3A	$H_{1.00}$	0.229(4)	1/4	-0.461(16)	0.03(2)*
НЗВ	$H_{1.00}$	0.017(4)	1/4	0.240(13)	0.010(17)*

Table 6. Selected bond distances (in Å) for suenoite.

M4	-O4B	2.066(3)	M1	-O1B	2.078(3)	M2	-O4A	2.030(3)	M3	-ОНЗА	2.066(4)
	-O4A	2.101(3)		-O1A	2.082(3)		-O4B	2.034(3)		-ОНЗВ	2.073(4)
	-O2B	2.178(3)		-ОНЗВ	2.093(3)		-O2A	2.094(3)		-O1A	2.091(3)
	-O2A	2.197(3)		-ОНЗА	2.102(3)		-O2B	2.102(3)		-O1A	2.091(3)
	-O5A	2.449(3)		-O2A	2.128(3)		-O1A	2.150(3)		-O1B	2.097(3)
	-O6B	2.737(3)		-O2B	2.144(3)		-O1B	2.154(3)		-O1B	2.097(3)
	-O5B	2.968(3)									
< M	<i>1</i> 4–0>	2.385	< 1	M1-O>	2.104	< M	12-O>	2.094	< 1	M3-O>	2.086
	-O6B	3.417(3)									
<i>T</i> 1A	-O1A	1.614(3)	<i>T</i> 1B	-O1B	1.613(3)	T2A	-O4A	1.595(3)	T2B	-O4B	1.602(3)
	-O7A	1.6178(16)		-O7B	1.6207(16)		-O2A	1.620(3)		-O2B	1.624(3)
	-O6A	1.620(3)		-O6B	1.630(3)		-O6A	1.629(3)		-O5B	1.643(3)
	-O5A	1.636(3)		-O5B	1.632(3)		-O5A	1.670(3)		-O6B	1.658(3)
< T	1a-O>	1.622	< T	1B-O>	1.624	< T2	2A-O>	1.628	< T	'2B-O>	1.632

Electron microprobe data indicate the occurrence of minor Ca and Na at the A site, i.e. $Ca_{0.07}Na_{0.02}$. However, the single-crystal X-ray diffraction study does not provide any indication of the partial occupancy at this position, and the maximum residual in the difference-Fourier map is less than $1e \, \text{Å}^{-3}$, to be compared with an expected site-scattering value of ca. 1.6e. This minor discrepancy may be interpreted as the possible unobserved intergrowth of do-

mains of exsolved (Ca,Na)-amphiboles in the studied crystal of suenoite, as described for instance in cummingtonite- $(P2_1/m)$ by Hawthorne et al. (2025). On the other hand, the measured Ca may also occur as B cation, as its full attribution as A cation in the formula calculation is solely driven by the excess of (B+C) cations. This interpretation is supported by the absence of significant residual electron density

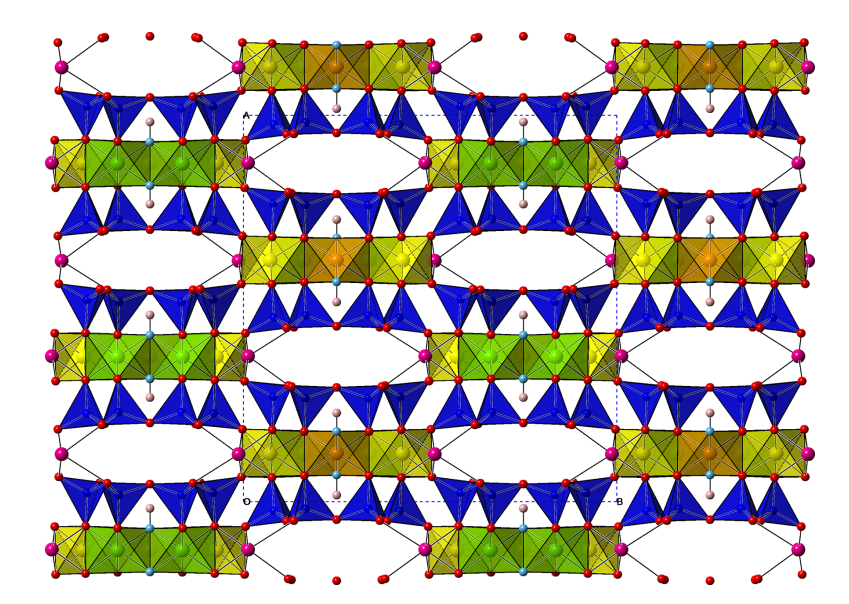


Figure 5. Crystal structure of suenoite, as seen down c. Symbols: blue polyhedra – S sites, green polyhedra – S sites, yellow polyhedra – S sites, orange polyhedra – S sites, magenta circles – S sites, red circles – S sites, light blue circles – S sites, pink circles – S sites. The unit cell is outlined as dotted lines.

Table 7. Refined and calculated site scattering (s.s., in electrons per formula unit) and proposed site population (in atoms per formula unit) for suenoite.

Site	Refined s.s.	Proposed site population	Calculated s.s.
M4	48.8	Mn _{1.64} Fe _{0.36}	50.4
M1	34.2	$Mg_{1.20}Mn_{0.60}Fe_{0.20}$	34.6
M2	29.7	$Mg_{1.60}Fe_{0.40}$	29.6
M3	15.7	$Mg_{0.75}Fe_{0.25}$	15.5

 $(> 1 e \text{ Å}^{-3})$ at the A site position in the difference-Fourier map, suggesting no unaccounted for cation occupancy.

The octahedral strip, formed by the M1, M2, and M3polyhedra, hosts Mg, Mn²⁺, and Fe²⁺. The site population at the M1, M2, and M3 sites was proposed on the basis of the refined site scattering and the spectroscopic data. Raman spectroscopy data suggest a total amount of 1.32 ^CFe²⁺ apfu, with the sum of Fe²⁺ at M1 and M3 of 0.93 apfu and, consequently, 0.39 Fe^{2+} at the M2 site. These values were derived using a relation proposed by Waeselmann et al. (2019) for ^CMn-free amphiboles. However, even if the total amount of Fe²⁺, measured through electron microprobe data, 1.27 apfu, is in agreement with the predicted value, Mössbauer data suggest that 28 % of Fe^{2+} is at M4. Consequently, the values obtained using the relation of Waeselmann et al. (2019) were interpreted as giving the total sum of ^C(Fe,Mn). Then, in agreement with Oberti et al. (2018), Mn was distributed considering the site preference $M1 > M2 \gg M3$. Indeed, the larger amount of Mn^{2+} at the M1 site is consistent with the relatively larger < M1-O> distance with respect to the other two octahedra. The proposed site populations at the M1-M3 sites result in calculated site-scattering values which closely match the refined site-scattering values obtained by free refinement of the occupancy (Table 7). Overall, the total site-scattering value at M1+M2+M3 is 79.6 e (from the refined site occupancies) vs. 79.7 e (from the proposed site populations). Bond-valence sums at the M1-M3 sites range between 2.10 and 2.18 valence units (v.u.) (Table 8).

The M4 site, at the junction between the strips of octahedra and the double chains of tetrahedra, has five bond distances shorter than 2.50 Å and two additional longer ones (up to 2.97 Å). The eighth O atom is at a very long distance of 3.417 Å. The site population was based on both refined site scattering (Table 7) and the results of Mössbauer spectroscopy, indicating the partial replacement of Mn^{2+} by Fe^{2+} . The bond-valence sum at the M4 site is 1.83 v.u., in accordance with the occurrence of divalent cations.

The T sites are mainly occupied by Si; in accordance with chemical data, only minor Al occur. Average < T–O> distances range from 1.622 to 1.632 Å, whereas the $\ll T$ –O> distance is 1.6265 Å. Following the relationship between the $\ll T$ –O> and the content of $^{[4]}$ Al (Hawthorne and Oberti, 2007), this latter value should be around 0.3 Al apfu, larger than the value found in electron microprobe analysis, i.e. 0.06 Al apfu. However, bond-valence sums at the T sites vary between 3.92 and 4.03 v.u., in accordance with an almost full occupancy by Si.

Finally, bond-valence sums of O atoms are in the range 1.92–2.07 v.u., the only exception being represented by the atoms at the OH3A and OH3B that have bond-valence sums of 1.10 and 1.11 v.u., respectively, in agreement with their occupancy by (OH) groups.

Table 8. Bond-valence balance (in valence unit) for suenoite.

Site	M4	<i>M</i> 1	M2	М3	T1A	<i>T</i> 1B	T2A	T2B	$\Sigma_{ m anions}$
O1A		0.39	0.30	0.35 ^{↓×2}	1.03				2.07
O1B		0.39	0.29	$0.35^{\downarrow \times 2}$		1.03			2.06
O2A	0.32	0.34	0.35				1.01		2.02
O2B	0.34	0.33	0.34					1.00	2.01
OH3A		$2 \times \rightarrow 0.36$		0.38					1.10
OH3B		$^{2\times\rightarrow}0.37$		0.37					1.11
O4A	0.42		0.41				1.08		1.92
O4B	0.46		0.41					1.06	1.95
O5A	0.16				0.97		0.88		2.02
O5B	0.04					0.98		0.95	1.97
O6A	0.01				1.01		0.99		2.01
O6B	0.08					0.98		0.91	1.97
O7A					$2 \times \rightarrow 1.02$				2.04
O7B						$2 \times \rightarrow 1.01$			2.02
$\Sigma_{cations}$	1.83	2.18	2.10	2.15	4.03	4.00	3.96	3.92	

Note: left and right superscripts indicate the number of equivalent bonds involving anions and cations, respectively. For sites with mixed occupancy, the bond valences have been weighted according to the site population given in Table 7.

Table 9. Valid orthorhombic *Pnma* amphibole-supergroup minerals.

Species	Ideal formula	a (Å)	b (Å)	c (Å)	$V(\mathring{\rm A}^3)$	Ref.
Magnesium-iron-mangar	nese amphiboles					
Anthophyllite	$A \square B Mg_2 C Mg_5(Si_8O_{22})(OH)_2$	18.54	18.03	5.28	1765.6	[1]
Ferro-anthophyllite	$^{A}\Box ^{B}\mathrm{Fe}_{2}^{2+} {^{C}}\mathrm{Fe}_{5}^{2+}(\mathrm{Si}_{8}\mathrm{O}_{22})(\mathrm{OH})_{2}$	18.69	18.36	5.34	1830.3	[2]
Ferro-gedrite	$A \square B \operatorname{Fe}_{2}^{2+} C(\operatorname{Fe}_{3}^{2+} \operatorname{Al}_{2})(\operatorname{Al}_{2}\operatorname{Si}_{6}\operatorname{O}_{22})(\operatorname{OH})_{2}$	18.60	17.69	5.32	1751.5	[3]
Ferro-papikeite	${}^{A}\text{Na}{}^{B}\text{Fe}_{2}^{2+}{}^{C}(\text{Fe}_{3}^{2+}\text{Al}_{2})(\text{Al}_{3}\text{Si}_{5}\text{O}_{22})(\text{OH})_{2}$	18.63	17.89	5.30	1767.2	[4]
Gedrite	$A \square B \operatorname{Mg2}^{C}(\operatorname{Mg3Al_2})(\operatorname{Al_2Si_6O_{22}})(\operatorname{OH})_2$	18.54	17.81	5.27	1740.4	[5]
Papikeite	A Na B Mg ₂ C (Mg ₃ Al ₂)(Al ₃ Si ₅ O ₂₂)(OH) ₂	18.63	17.85	5.28	1756.3	[6]
Suenoite	$^{A}\square$ B Mn ₂ C Mg ₅ (Si ₈ O ₂₂)(OH) ₂	18.75	18.14	5.32	1808.6	[7]
Lithium amphiboles						
Ferro-ferri-holmquistite	$^{A}\Box ^{B}\text{Li}_{2} ^{C}(\text{Fe}_{3}^{2+}\text{Fe}_{2}^{3+})(\text{Si}_{8}\text{O}_{22})(\text{OH})_{2}$	18.54	17.92	5.31	1765.5	[8]
Ferro-holmquistite	$^{A}\Box ^{B}\text{Li}_{2} ^{C}(\text{Fe}_{3}^{2}+\text{Al}_{2})(\text{Si}_{8}\text{O}_{22})(\text{OH})_{2}$	18.29	17.68	5.28	1706.6	[9]
Holmquistite	$^{A}\square ^{B}\operatorname{Li}_{2}{^{C}}(\operatorname{Mg}_{3}\operatorname{Al}_{2})(\operatorname{Si}_{8}\operatorname{O}_{22})(\operatorname{OH})_{2}$	18.36	17.75	5.29	1724.0	[10]

⁽¹⁾ Walitzi et al. (1989), (2) Popp et al. (1976), (3) Matsubara et al. (1980), (4) Hawthorne et al. (2022), (5) Nestola et al. (2012), (6) Kihle et al. (2023), (7) this work, (8) Nagashima et al. (2022), (9) Cámara and Oberti (2005), and (10) Vogt et al. (1958).

6.2 Suenoite in the frame of amphibole-supergroup minerals

Suenoite is a new addition to the *Pnma* amphiboles (Table 9). The 10 species currently known belong to different amphibole subgroups and occur in different geological environments.

Suenoite belongs to the subgroup of magnesium-iron-manganese amphiboles (Hawthorne et al., 2012), along with anthophyllite, ferro-anthophyllite, gedrite, ferro-gedrite, ferro-papikeite, and papikeite. These latter minerals usually occur in medium- to high-grade metamorphic rocks (e.g. Rabbitt, 1948; Klein, 1966; Ford and Skippen, 1997; Elliot-

Meadows et al., 2000; Peck and Valley, 2000; Hinchey and Carr, 2007; Hawthorne et al., 2022; Kihle et al., 2023). Suenoite occurs in a Mn ore deposit metamorphosed under greenschist-facies conditions (e.g. Molli et al., 2002; Fellin et al., 2007). The monoclinic dimorph clino-suenoite has been found in a similar geological setting, i.e. a metamorphosed Mn mineralisation (Oberti et al., 2018); a monoclinic amphibole, whose chemical composition based on energy-dispersive spectroscopy data is the same as that of clino-suenoite, has also been found at the Scortico–Ravazzone ore deposit and is currently under investigation.

The remaining three *Pnma* amphiboles belong to the subgroups of lithium amphiboles. These amphiboles typically

crystallise owing to the interaction between Li-rich fluids and country rocks. Holmquistite is a grandfathered member of the amphibole supergroup, having been described at the beginning of the 20th century (Osann, 1913), whereas the other two Fe-bearing species, ferro-holmquistite and ferro-ferri-holmquistite, have been described since the beginning of the 21st century (Cámara and Oberti, 2005; Nagashima et al., 2022).

As stated above, the root name suenoite was first adopted for the mineral proto-ferro-suenoite, the third known mineral of the amphibole supergroup denoted by the prefix "proto-", i.e. having *Pnmn* symmetry, after proto-ferro-anthophyllite (Sueno et al., 1988) and proto-anthophyllite (Konishi et al., 2003).

7 Conclusion

Suenoite is a new member of the amphibole supergroup. It is the first Pnma amphibole with $^B(Mn^{2+})_2$. Manganese amphiboles are not uncommon as accessory phases in several metamorphosed Mn mineralisations. At the Scortico–Ravazzone ore deposit, several fibrous minerals, some of which are already identified as members of the amphibole supergroup, occur. Their study is currently underway, and it will improve our understanding of amphibole crystal chemistry.

Suenoite is the second mineral species with its type locality at the Scortico–Ravazzone ore deposit, following the discovery of the Mn-nesosilicate scorticoite (Biagioni et al., 2019). Its discovery, along with the recent description of other interesting species (e.g. melanostibite – Musetti et al., 2022), suggests the necessity of an accurate mineralogical investigation of the different mineral assemblages occurring at this hitherto neglected Italian locality.

Data availability. The crystallographic information file of suenoite is available in the Supplement.

Supplement. The supplement related to this article is available online at https://doi.org/10.5194/ejm-37-761-2025-supplement.

Author contributions. CB carried out single-crystal X-ray diffraction and micro-Raman spectroscopy. UH collected optical, infrared, and Mössbauer data. FB performed electron microprobe analysis. CB, MP, and EB critically examined the data. CB and MP wrote the paper, with inputs from the other authors.

Competing interests. At least one of the (co-)authors is a member of the editorial board of *European Journal of Mineralogy*. The peer-review process was guided by an independent editor, and the authors also have no other competing interests to declare.

Disclaimer. Publisher's note: Copernicus Publications remains neutral with regard to jurisdictional claims made in the text, published maps, institutional affiliations, or any other geographical representation in this paper. While Copernicus Publications makes every effort to include appropriate place names, the final responsibility lies with the authors.

Acknowledgements. Tiberio Bardi is acknowledged for providing us with the specimen of suenoite used for this mineralogical investigation. Vladimir Krivovichev and the anonymous reviewer are thanked for their useful comments.

Financial support. This research has been supported by the Ministero dell'Istruzione, dell'Università e della Ricerca through the project PRIN 2020 "HYDROX – HYDRous-vs OXo-components in minerals: adding new pieces to the Earth's H₂O cycle puzzle", prot. 2020WYL4NY.

Review statement. This paper was edited by Sergey Krivovichev and reviewed by Vladimir Krivovichev and one anonymous referee.

References

Abrecht, J.: Manganiferous phyllosilicate assemblages: occurrences, compositions and phase relations in metamorphosed Mn deposits, Contr. Mineral. Petrol., 103, 228–241, 1989.

Banno, Y., Momma, K., Miyawaki, R., and Yamada, S.: New data on ferri-ghoseite in Sanbagawa quartz schist from the Iimori region, Wakayama Prefecture, Japan: solid solution between magnesio-riebeckite and clino-suenoite, J. Mineral. Petrol. Sci., 114, 33–40, 2019.

Barkley, M. C., Yang, H., and Downs, R. T.: Kôzulite, an Mn-rich alkali amphibole, Acta Crystallogr., E66, i83, https://doi.org/10.1107/S1600536810046015, 2010.

Biagioni, C., Bonaccorsi, E., Kampf, A. R., Zaccarini, F., Hålenius, U., and Bosi, F.: Scorticoite, IMA 2018-159, CNMNC Newsletter No. 49, Mineral. Mag., 83, 479–483, 2019.

Brese, N. E. and O'Keeffe, M.: Bond-valence parameters for solids, Acta Crystallogr., B47, 192–197, 1991.

Bruker AXS Inc.: APEX 3. Bruker Advanced X-ray Solutions, Madison, Wisconsin, USA, 2016.

Cámara, F. and Oberti, R.: The crystal-chemistry of holmquistites: Ferroholmquistite from Greenbushes (Western Australia) and hints for compositional constraints in ^BLi amphiboles, Am. Mineral., 90, 1167–1176, 2005.

Di Sabatino, B.: Su una paragenesi del giacimento manganesifero di Scortico (Alpi Apuane), Period. Mineral., 36, 965–992, 1967.

Elliot-Meadows, S. R., Froese, E., and Appleyard, E. C.: Cordierite – anthophyllite – cummingtonite rocks from the Lar deposit, Laurie Lake, Manitoba, Can. Mineral., 38, 545–550, 2000.

Fellin, M. G., Reiners, P. W., Brandon, M. T., Wuthrich, E., and Balestrieri, M. L.: Thermochronologic evidence for exhumational history of the Alpi Apuane metamorphic core complex, northern Apennines, Italy, Tectonics, 26, TC6015, https://doi.org/10.1029/2006TC002085, 2007.

- Ford, F. D. and Skippen, G. B.: Petrology of the Flinton Creek metaperidotites: enstatite magnesite and anthophyllite magnesite assemblages from the Grenville Province, Can. Mineral., 35, 1221–1236, 1997.
- Hawthorne, F. C.: Mössbauer spectroscopy, in: Spectroscopic Methods in Mineralogy and Geology, ed. F.C. Hawthorne, Rev. Mineral., 18, 255–340, 1988.
- Hawthorne, F. C. and Della Ventura, G.: Short-range order in amphiboles, Rev. Mineral. Geochem., 67, 173–222, 2007.
- Hawthorne, F. C., Oberti, R., Cannillo, E., Sardone, N., Zanetti, A., Grice, J. D., and Ashley, P. M.: A new anhydrous amphibole from the Hoskins mine, Grenfell, New South Wales, Australia: Description and crystal structure of ungarettiite, NaNa₂(Mn₂²⁺Mn₃³⁺)Si₈O₂₂O₂, Am. Mineral., 80, 165–172, 1995a.
- Hawthorne, F. C., Ungaretti, L., and Oberti, R.: Site populations in minerals: terminology and presentation of results of crystalstructure refinement, Can. Mineral., 33, 907–911, 1995b.
- Hawthorne, F. C., and Oberti, R.: Classification of the amphiboles, Rev. Mineral. Geochem., 67, 55–88, 2007.
- Hawthorne, F. C., Oberti, R., Harlow, G. F., Maresch, W. V., Martin, R. F., Schumacher, J. C., and Welch, M. D.: Nomenclature of the amphibole supergroup, Am. Mineral., 97, 2031–2048, 2012.
- Hawthorne, F. C., Day, M. C., Fayek, M., Linthout, K., Lustenhouwer, W. J., and Oberti, R.: Ferro-papikeite, ideally NaFe₂²⁺(Fe₃²⁺Al₂)(Si₅Al₃)O₂₂(OH)₂, a new orthorhombic amphibole from Nordmark (Western Bergslagen), Sweden: Description and crystal structure, Am. Mineral., 107, 306–312, 2022.
- Hawthorne, F. C., Lapierre, A. R., Abdu, Y., Oberti, R., and Day, M. C.: Cummingtonite-(P2₁/m): Crystal structure refinement, Mössbauer spectroscopy and infrared spectroscopy, and some aspects of classification of magnesium-iron-manganese amphiboles, Mineral. Mag., 89, 411–420, https://doi.org/10.1180/mgm.2025.14, 2025.
- Hinchey, A. M. and Carr, S. D.: Protolith composition of cordierite
 gedrite basement rocks and garnet amphibolite of the Bearpaw
 Lake area of the Thor-Odine dome, Monashee Complex, British
 Columbia, Canada. Can. Mineral., 45, 607–629, 2007.
- Holtstam, D., Cámara, F., Skogby, H., and Karlsson, A.: Hjalmarite, a new Na-Mn member of the amphibole supergroup, from Mn skarn in the Långban deposit, Värmland, Sweden, Eur. J. Mineral., 31, 565–574, 2019.
- Holtstam, D., Cámara, F., Skogby, H., De Leo, A., and Karlsson, A.: Clino-ferro-suenoite, IMA 2024-032, in: CNMNC Newsletter 81, Eur. J. Mineral., 36, https://doi.org/10.5194/ejm-36-917-2024, 2024.
- Kihle, J. B., Day, M. C., and Hawthorne, F. C.: Papikeite, IMA 2022-145, in: CNMNC Newsletter 74, Eur. J. Mineral., 35, https://doi.org/10.5194/ejm-35-659-2023, 2023.
- Klein, C.: Mineralogy and petrology of the metamorphosed Wabush Iron Formation, Southwestern Labrador, J. Petrol., 7, 246–305, 1966.
- Konishi, H., Groy, T. L., Dódony, I., Miyawaki, R., Matsubara, S., and Buseck, P. R.: Crystal structure of protoanthophyllite: A new mineral from the Takase ultramafic complex, Japan, Am. Mineral., 88, 1718–1723, 2003.
- Kraus, W. and Nolze, G.: PowderCell a program for the representation and manipulation of crystal structures and calculation

- of the resulting X-ray powder patterns, J. Appl. Crystallogr., 29, 301–303, 1996.
- Mandarino, J. A.: The Gladstone-Dale relationship. Part IV. The compatibility concept and its application, Can. Mineral., 19, 441–450, 1981.
- Matsubara, S., Kato, A., and Nomura, M.: The occurrence of ferrogedrite from the Kawai mine, Ena, Gifu Prefecture, Japan, Bull. Natl. Sci. Mus. Tokyo Ser., C6, 107–113, 1980.
- Molli, G., Giorgetti, G., and Meccheri, M.: Tectono-metamorphic evolution of the Alpi Apuane Metamorphic Complex: new data and constraints for geodynamic model, Boll. Soc. Geol. Ital., 1, 789–800, 2002.
- Musetti, S., Biagioni, C., Hålenius, U., Bonaccorsi, E., and Zaccarini, F.: New data on melanostibite, Mn₂Fe³⁺Sb⁵⁺O₆, Mineral. Mag., 86, 903–909, 2022.
- Nagashima, M., Imaoka, T., Kano, T., Kimura, J., Chang, Q., and Matsumoto, T.: Ferro-ferri-holmquistite, $\Box \text{Li}_2(\text{Fe}_3^{2+}\text{Fe}_2^{3+}) \text{Si}_8\text{O}_{22}(\text{OH})_2$, $\text{Fe}^{2+}\text{Fe}^{3+}$ analogue of holmquistite, from the Iwagi islet, Ehime, Japan, Eur. J. Mineral., 34, 425–438, https://doi.org/10.5194/ejm-34-425-2022, 2022.
- Nambu, M., Tanida, K., and Kitamura, T.: Kôzulite, a new alkali amphibole, from Tanohata Mine, Iwate Prefecture, Japan, J. Japan. Ass. Mineral. Petrol. Econ. Geol., 62, 311–328, 1969 (in Japanese).
- Nestola, F., Pasqual, D., Welch, M. D., and Oberti, R.: The effects of composition upon the high-pressure behaviour of amphiboles: compression of gedrite to 7 GPa and a comparison with anthophyllite and proto-amphibole, Am. Mineral., 76, 987–995, 2012.
- Oberti, R. and Ghose, S.: Crystal chemistry of a complex Mnbearing alkali amphibole ("tirodite") on the verge of exsolution, Eur. J. Mineral., 5, 1153–1160, 1993.
- Oberti, R., Della Ventura, G., Boiocchi, M., Zanetti, A., and Hawthorne, F. C.: The crystal chemistry of oxo-mangani-leakeite and mangano-mangani-ungarettiite from the Hoskins mine and their impossible solid solutions: An XRD and FTIR study, Mineral. Mag., 81, 707–722, 2017.
- Oberti, R., Boiocchi, M., Hawthorne, F. C., Ciriotti, M. E., Revheim, O., and Bracco, R.: Clino-suenoite, a newly approved magnesium-iron-manganese amphibole from Valmalenco, Sondrio, Italy, Mineral. Mag., 82, 189–198, 2018.
- Osann, A.: Über Holmquistit, eined Lithionglaukophan von der Insel Utö, Sitz. Heidl. Akad. Wissen., 1913, 3–16, 1913.
- Peck, W. H. and Valley, J. W.: Genesis of cordierite gedrite gneisses, Central Metasedimentary Belt boundary thrust zone, Grenville Province, Ontario, Canada, Can. Mineral., 38, 511– 524, 2000.
- Popp, R. K., Gilbert, M. C., and Craig, J. R.: Synthesis and X-ray properties of Fe-Mg orthoamphiboles, Am. Mineral., 61, 1267– 1279, 1976.
- Pouchou, J. L. and Pichoir, F.: "PAP" (φρ Z) procedure for improved quantitative microanalysis, in: Microbeam Analysis, edited by: Armstrong, J. T., 104–106, San Francisco Press, San Francisco, 1985.
- Prescher, C., McCammon, C., and Dubrovinsky, L.: MossA: a program for analyzing energy-domain Mössbauer spectra from conventional and synchrotron sources, J. Appl. Crystallogr., 45, 329–331, 2012.

- Rabbitt, J. C.: A new study of the anthophyllite series, Am. Mineral., 33, 263–323, 1948.
- Sheldrick, G. M.: Crystal structure refinement with SHELXL, Acta Crystallogr., C71, 3–8, 2015.
- Sueno, S., Matsuura, S., Gibbs, G. V., and Boisen Jr., M. B.: A crystal chemical study of protoanthophyllite: orthoamphiboles with the protoamphibole structure, Phys. Chem. Miner., 25, 366–377, 1988.
- Sueno, S., Matsuura, S., Bunno, M., and Kurosawa, M.: Occurrence and crystal chemical features of protoferro-anthophyllite and protomangano-ferroanthophyllite from Cheyenne Canyon and Cheyenne Mountain, U.S.A. and Hirukawa-mura, Suishoyama, and Yokone-yama, Japan, J. Mineral. Petrol. Sci., 97, 127–136, 2002.
- Vogt, T., Bastiansen, O., and Skancke, P.: Holmquistite as a rhombic amphibole, Am. Mineral., 43, 981–982, 1958.

- Waeselmann, N., Schlüter, J., Malcherek, T., Della Ventura, G., Oberti, R., and Mihailova, B.: Nondestructive determination of the amphibole crystal-chemical formulae by Raman spectroscopy: One step closer, J. Raman Spectr., 51, 1530–1548, 2019.
- Walitzi, E. M., Walter, F., and Ettinger, K.: Verfeinerung der kristallstruktur von anthophyllit vom Ochsenkogel/Gleinalpe, Osterreich, Z. Kristallogr., 188, 237–244, 1989.
- Williams, P. A. Hatert, F., Pasero, M., and Mills, S. J.: IMA Commission on New Minerals, Nomenclature and Classification (CN-MNC) Newsletter 16 New minerals and nomenclature modifications approved in 2013, Mineral. Mag., 77, 2695–2709, 2013.
- Wilson, A. J. C. (Ed.): International Tables for Crystallography, Volume C: Mathematical, physical and chemical tables, Kluwer Academic, Dordrecht, NL, 1992.